Designed to penetrate: Time-resolved interaction of single antibiotic molecules with bacterial pores

Ekaterina M. Nestorovich*, Christophe Danelon†, Mathias Winterhalter†, and Sergey M. Bezrukov*‡§

*Laboratory of Physical and Structural Biology, National Institute of Child Health and Human Development, National Institutes of Health, Building 9, Room 1E-122, Bethesda, MD 20892-0924; †Institut Pharmacologie et Biologie Structurale, 31 077 Toulouse, France; and ‡St. Petersburg Nuclear Physics Institute, Gatchina 188350, Russia

Edited by Charles F. Stevens, The Salk Institute for Biological Studies, La Jolla, CA, and approved May 28, 2002 (received for review April 3, 2002)

Membrane permeability barriers are among the factors contributing to the intrinsic resistance of bacteria to antibiotics. We have been able to resolve single ampicillin molecules moving through a channel of the general bacterial porin, OmpF (outer membrane protein F), believed to be the principal pathway for the β-lactam antibiotics. With ion channel reconstitution and high-resolution conductance recording, we find that ampicillin and several other efficient penicillins and cephalosporins strongly interact with the residues of the constriction zone of the OmpF channel. Therefore, we hypothesize that, in analogy to substrate-specific channels that evolved to bind certain metabolite molecules, antibiotics have ''evolved'' to be channel-specific. Molecular modeling suggests that the charge distribution of the ampicillin molecule complements the charge distribution at the narrowest part of the bacterial porin. Interaction of these charges creates a region of attraction inside the channel that facilitates drug translocation through the constriction zone and results in higher permeability rates.

Although the mechanisms of antibiotic action on organisms are not completely understood, an essential step for most drugs is their translocation across the target membrane (1). Now, that the ''golden age'' of antibiotics is considered to be over (ref. 2, but see ref. 3), the search for new effective antibiotics is even more important. Many of the antibacterial and antifungal drugs are derived from bacteria or molds, but a growing number of new antibiotics originate in *de novo* synthesis, where the ability to predict the drug potency is of particular significance. In many important cases (1) membrane permeability barriers coupled with drug efflux systems or with the presence of periplasmic β-lactamases are recognized among the key factors for the intrinsic resistance of bacteria to antibiotics (4).

The general diffusion porin OmpF (outer membrane protein F) of *Escherichia coli* is believed to be the principal pathway for β-lactam antibiotics. *In vivo* assays of some β-lactam-resistant strains of *E. coli* have shown a deficient OmpF production (5). These observations have led researchers to conclude on the importance of OmpF for drug permeation and motivated previous intensive studies of OmpF channels (6). Recent work (7) has demonstrated that modification of the primary structure of OmpF in the region of its third loop could change sensitivity of bacteria to antibiotics.

Fig. 1 illustrates antibiotic molecules passing through the trimeric OmpF channel. This is the pathway from the outside medium into the periplasmic space of bacteria where β-lactam antibiotics inhibit the cell-wall biosynthesis by binding to transpeptidase and preventing the crosslinking of the peptidoglycan layer (8).

Methods

Chemicals. Wild-type OmpF was isolated and purified from an *E. coli* culture as described elsewhere (9). The following chemical reagents were used: ampicillin anhydrate (Sigma); KCl, KOH, and HCl (Mallinckrodt); $CaCl_2$ (Quality Biologicals, Gaithersburg, MD); ultrol-grade Mes or Hepes (Calbiochem); ''purum'' hexadecane (Fluka); diphytanoyl phosphatidylcholine (DPhPC) (Avanti Polar Lipids); and pentane (Burdick and Jackson).

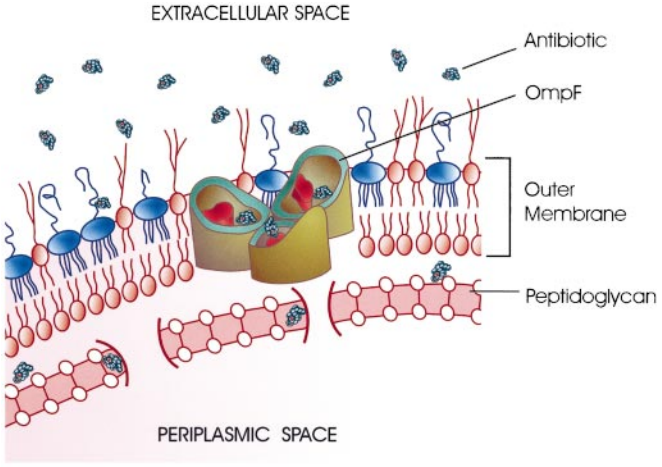

Fig. 1. A trimeric OmpF channel in the lipid bilayer of the outer bacterial membrane is a pathway for penicillin antibiotics to the periplasmic space. For simplicity, the inner glycerophospholipid bilayer of the double membrane of Gram-negative bacteria is not shown. Between the inner and the outer membranes there is a thin, rigid, highly porous layer of peptidoglycan that surrounds and protects bacteria cells mechanically. Peptidoglycan is the main target of β-lactam antibiotics. These drugs are structural analogues of the terminal D-alanyl-D-alanine unit that participates in peptidoglycan synthesis and are able to interrupt the process eventually leading to bacteria death.

Channel Reconstitution. ''Solvent-free'' bilayer lipid membranes were formed as described elsewhere (10). The film and the membrane capacitances were close to 25 pF each. Single channels were formed by adding 0.1–0.3 μl of 1 μg ml^{-1} stock solution of OmpF to 1.5 ml aqueous phase in the cis half of the chamber. The single-channel measurements were carried out at room temperature of 23 ± 2°C in solutions containing 1 mM $CaCl_2$ with KCl concentration equal to (0.01 ÷ 2.1) M at pH 3–11. With this protocol, we have found that OmpF insertion was predominantly directional [similar results were recently reported for maltoporin (11)]. Our observation is based on the asymmetry of channel conductance that is lower at the transmembrane potential difference of +200 mV (that is, when applied potential is more positive at the side of OmpF addition) than at −200 mV, at pH 7. In 1 M and 0.1 M KCl, this difference was about 4% and 35%, respectively, and was used as a control of the insertion direction.

Molecular Modeling. Simulations were carried out on a Silicon Graphics workstation by using the CVFF (consistent valence

This paper was submitted directly (Track II) to the PNAS office.

§To whom reprint requests should be addressed. E-mail: bezrukov@helix.nih.gov.

force field) in the INSIGHT II 98 and DISCOVER programs (Biosym, Micron Separations). We used the structural model of the wild-type OmpF determined at 2.4 Å resolution (12) as the starting structure for the porin monomer. The lumen of the channel was filled with water molecules and the main-chain C^{α} atoms were constrained at their crystallographic positions during refinement calculations. The ampicillin molecule was built in its zwitterionic form and was docked at the constriction zone of the channel to satisfy experimental observations. The energy of the entire system was minimized with the conjugated gradients method.

Results

In an attempt to characterize and quantify the drug transfer rate we have reconstituted purified OmpF into planar lipid membranes and studied its single channels in the presence of a β-lactam antibiotic, ampicillin. It is well known that substrate-specific channels such as sugar-specific maltoporin or LamB (13–15) have evolved to bind corresponding substrates to facilitate their transport into the cell. In fact, in the case of LamB this binding is so strong (16) that recently it has become possible to detect translocation of single sugar molecules (11, 17) analogously to "stochastic sensing" of water-soluble analytes (18, 19).

Is the interaction between effectively penetrating drugs and the outer membrane channel strong enough to render the passage events resolvable? Yes, it is. Typical recordings of ion currents through OmpF trimers are shown in Fig. 2. A single OmpF channel spontaneously inserts as an oriented trimer (see *Methods*) with no visible "gating" at −100 mV of applied voltage (Fig. 2 *Top*). Addition of ampicillin (1–28 mM) to membrane-bathing solution on both sides of the membrane introduces vigorous fluctuations in the current through a single OmpF channel (Fig. 2 *Middle*). Increasing the time resolution to 15 μs allows us to resolve single-molecule ampicillin binding to OmpF as the fast transients between a fully open channel and 2/3 of channel conductance. We conclude that these stepwise transitions reflect the complete blockage of one of the monomers in the channel trimer.

An increase in the drug concentration increases the number of blockage events (Fig. 2 *Bottom*). The higher time resolution allows us to detect instances when single-molecule events of individual monomer blockage overlap in time. In these cases, the channel current is reduced to 1/3 of its initial value.

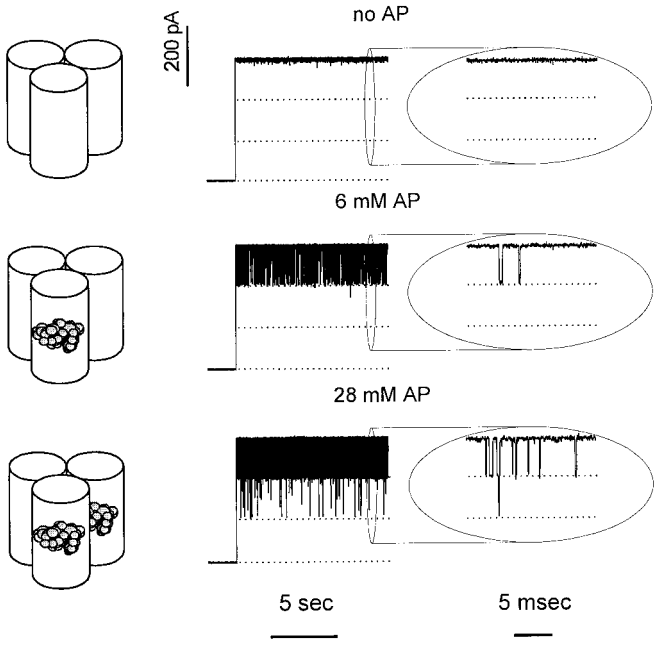

Fig. 2. Penetrating ampicillin (AP) molecules modulate ion current through a single OmpF channel reconstituted in a planar bilayer. Membrane bathing solution was 1 M KCl (pH 6.0), and the applied voltage was −100 mV. (*Top*) In the absence of antibiotic the ion movement is mainly determined by the geometry and the surface properties of the channel pore. The ion current is stable; no interruptions are seen even at the high resolution recording shown on the right. (*Middle*) In the presence of ampicillin in small concentrations one of the three OmpF pores gets spontaneously blocked by a translocating drug molecule. At the time resolution of 0.15 ms (*Left*) blockage events look like downward spikes. At the higher resolution of 0.015 ms (*Right*) they are seen as well defined steps to 2/3 of the open channel current and back. Time between blockage events and their width report on both thermodynamic and kinetic parameters of antibiotic–pore interactions. (*Bottom*) At higher ampicillin concentrations channel blockades are more frequent. Sometimes they statistically overlap in time, leading to transient reduction of ion current to 1/3 of its initial value.

Kinetic Analysis. If these stepwise fluctuations reflect ampicillin permeation into the channel then chemical rate equations provide a necessary tool to deduce the underlying thermodynamic and kinetic parameters of the antibiotic translocation. Statistical analysis of drug-induced fluctuations by either power spectral-density method (Fig. 3*A*) or by direct single-exponential fitting of blockage time histograms (Fig. 3*A Inset*) shows that the residence time of antibiotic binding does not depend appreciably on the drug concentration, whereas the number of channel-blockage events per second is proportional to ampicillin bulk concentration (Fig. 3*B*). This observation means that only one antibiotic molecule takes part in each transient closure.

The rate of single-molecule binding events (number of events per second, ν) was found by either direct counting or by noise analysis based on the following. Assuming that ampicillin binding is a two-state Markovian process, the current spectral density for the drug-induced OmpF blockage noise per monomer can be written as (20)

$$S_m(f) = \frac{4(\Delta i)^2\tau^2}{\tau_r + \tau_0}\frac{1}{1 + (2\pi f\tau)^2}, \qquad [1]$$

where Δi is the total change in current as a result of a single-molecule blockage, f is the frequency, and τ is the correlation time of the system defined in terms of the average residence time of a drug molecule in the pore, τ_r, and the mean lifetime of a monomer in the open state between successive blockages, τ_0

$$\tau \equiv \frac{\tau_r\tau_o}{\tau_r + \tau_o}. \qquad [2]$$

Correlation time τ was obtained by fitting experimentally obtained spectra with the Lorentzian in Eq. **1**. In the low-frequency limit ($f \to 0$) the spectral density takes the following frequency-independent form

$$S_m(0) = 4\nu_m(\Delta i)^2\tau^2, \qquad [3]$$

where the number of single-molecule binding events per second per monomer is given by

$$\nu_m = \frac{1}{\tau_r + \tau_o}. \qquad [4]$$

Therefore,

$$\nu_m = \frac{S_m(0)}{4(\Delta i)^2\tau^2}. \qquad [5]$$

When binding to different monomers is independent, the total number of blockages for the whole trimer is $\nu = 3\nu_m$ and the

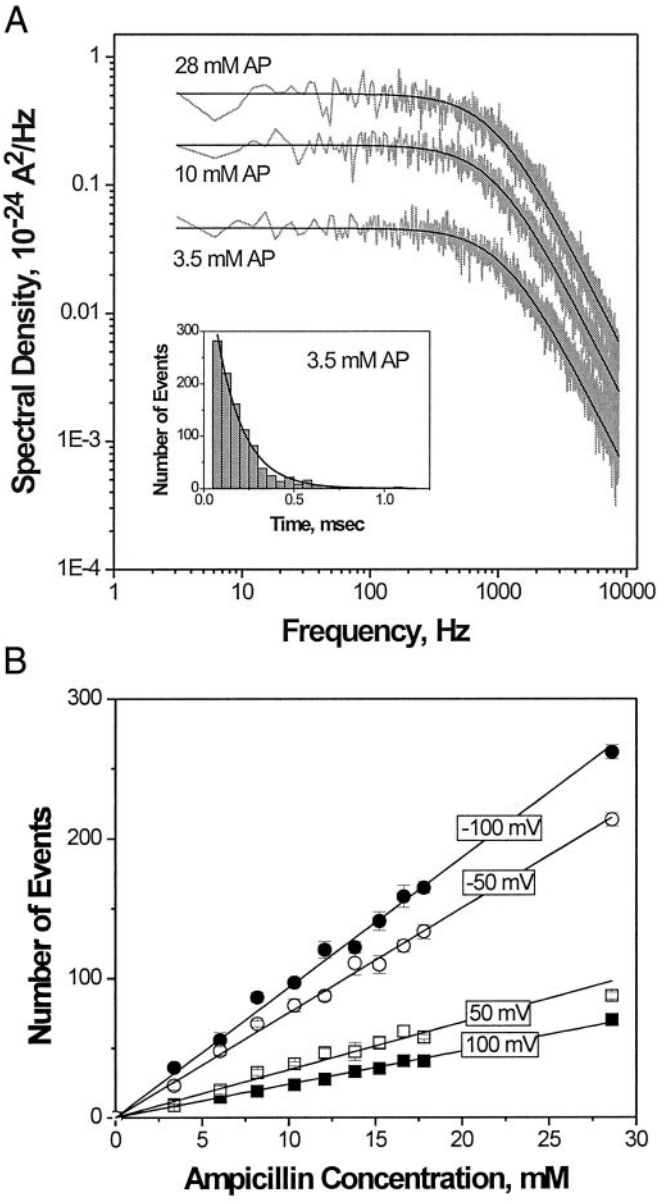

Fig. 3. (*A*) Power spectral densities of current fluctuations at three different ampicillin concentrations and distribution of dwell times in the blocked state (*Insert*) demonstrate that binding of drug is well described by a simple two-state Markovian process. Solid lines through the spectra are drawn according to Eq. **1** with $\tau = 1.41 \times 10^{-4}$ s; the solid line in the time histogram is an exponential fit with the characteristic time of 1.48×10^{-4} s. (*B*) The number of binding events per second, ν, is linear in ampicillin concentration and depends on applied voltage. For *A* the applied voltage was −100 mV. Membrane-bathing solution was 1 M KCl, pH 6.0, for *A* and *B*.

experimentally measured spectrum $S(0) = 3S_m(0)$, so that Eq. **5** can be used with the subscripts omitted. Both methods, i.e., direct counting and noise analysis, yielded identical results.

The average residence time of a drug molecule in the pore can be calculated according to (11)

$$\tau_r = \frac{\tau}{1-p}, \qquad [6]$$

where p is the equilibrium probability of finding a given monomer in the blocked state. In our experiments, p was always much smaller that unity, so that $\tau_r \approx \tau$. Again, the time histogram fitting and noise analysis methods gave results coinciding within the expected statistical error [compare $(1.41 \pm 0.09) \times 10^{-4}$ s obtained from the spectra in Fig. 3*A* with $(1.48 \pm 0.06) \times 10^{-4}$ s from the time histogram there].

The time-resolved transient blockage was also observed when ampicillin was added asymmetrically to either the cis or trans compartment of the cell. This finding suggests that an antibiotic molecule is able to enter the channel from both extracellular and intracellular openings. Statistical analysis has demonstrated that the average residence time, τ_r, remains identical regardless of whether the drug is added on the cis or trans side (Fig. 4*A*). This observation shows that once the drug molecule has entered the channel, it interacts with the same site. Therefore, we argue that approximately every second blockage reflects *translocation* of the molecule. The translocation vs. "same side binding-release" issue was recently discussed for the time-resolved binding of sugars to single maltoporin channels (11).

It is seen that both the residence time (Fig. 4*A*) and the event rate (Fig. 3*B*) are strong functions of voltage. A similar observation for sugar molecules and maltoporin channels (11) was tentatively explained by the effect of the applied electric field on geometry of the pore as a result of elasticity of the channel-forming protein. The authors hypothesized that small field-induced changes in pore geometry may cause large changes in binding because of the importance of the exact fit between the substrate molecular structure and the elements of the binding site.

To understand the mechanism of ampicillin interaction with OmpF we varied the pH of the bathing solutions. Fig. 4*B* shows dramatic changes in the frequency of binding events and a sharp maximum at pH 4.3 where $\nu = 280\ s^{-1}$. At 7.2 mM ampicillin concentration used in this experiment, the corresponding association rate constant *per monomer* is $k_{on} \approx \nu_m/[c] = \nu/(3[c]) = 1.3 \times 10^4\ (Ms)^{-1}$, where $[c]$ is the drug concentration. This value is orders of magnitude lower than diffusion-limited association rate constant for a molecule of this size. The reduced "on rate" probably reflects channel-imposed sterical hindrance or an energetically expensive desolvation step for the binding site access.

The equilibrium binding constant can be calculated according to

$$K = \frac{\nu_m \tau_r}{[c](1 - \nu_m \tau_r)}, \qquad [7]$$

and at −100 mV in 1 M KCl at pH 4.3 equals $(1.9 \pm 0.2)\ M^{-1}$. The strength of binding is sensitive to bathing solution salt concentration (see below). Reducing salt concentration to 0.1 M KCl leads to about a 20-fold increase in the binding constant. This value is still significantly smaller than the binding constant between maltooligosaccharides and maltoporin (11, 13–15, 16) but is close to the binding constant of ATP to VDAC (21), the mitochondrial porin.

The strong regulation of the binding rate by the solution pH can be understood by taking into consideration the ampicillin acid-base equilibrium. According to its pK values (22), the fraction of zwitterionic ampicillin reaches its maximum at ~pH 5. Cationic or anionic species of this antibiotic predominate in solution at lower or higher pH values. Although the rate peak is considerably sharper than the corresponding ion-zwitterion equilibrium [similar "accelerated titration" was recently found for mitochondrial porin (10)], the results suggest that the zwitterionic form of ampicillin interacts with the charged or polar residues inside the channel and that this interaction is favorable for the drug binding and translocation. This finding can explain the *in vivo* experiments of Rolinson and Stevens (23), indicating that ampicillin is about 10 times more active toward strains of *E. coli* in pH 5.5 than in pH 8 buffer.

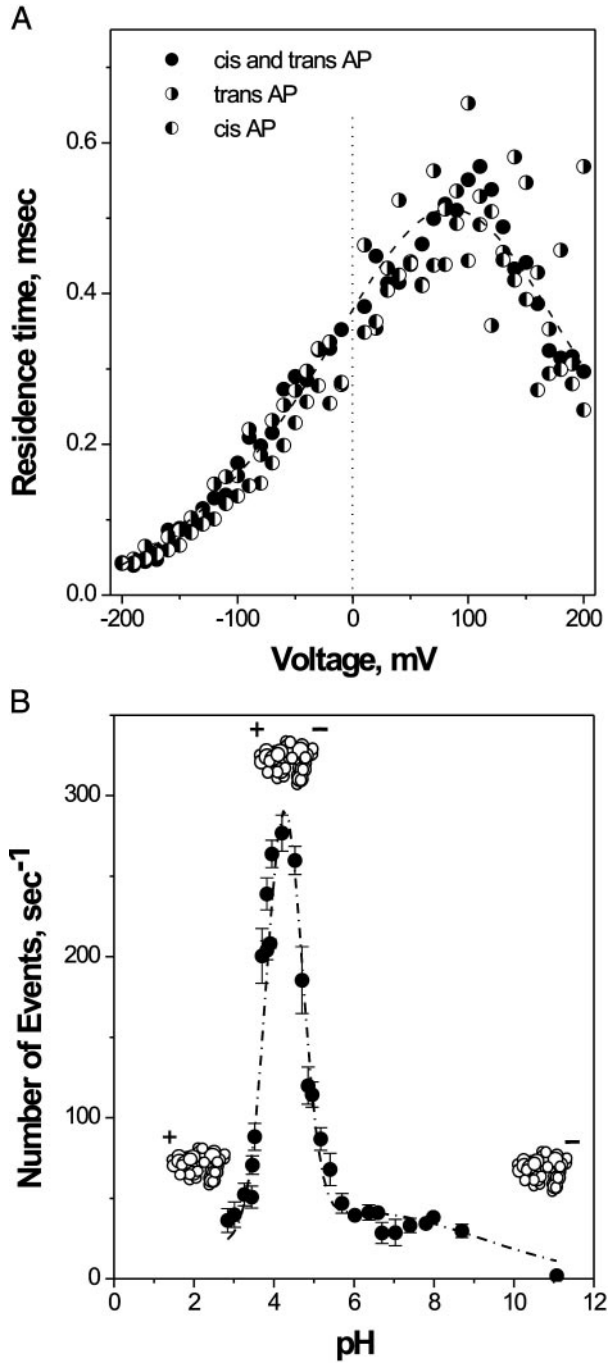

Fig. 4. (*A*) Over the whole range of applied voltages, the ampicillin residence time does not depend on the way of drug addition to the membrane-bathing solutions (cis, trans, or both sides). Filled circles represent experiments where antibiotic is added symmetrically; left-filled and right-filled circles correspond to cis and trans drug addition, respectively. The voltage dependence of the residence time shows a pronounced channel asymmetry. Ampicillin concentration was 11.5 mM, pH 6.0. (*B*) The number of ampicillin translocation events per second is a strong function of the bathing solution pH. The number of blockage events remains practically constant (at the rate of about $\nu = 40\ s^{-1}$) at pH from 6 to 9. At about pH 4.5 the rate peaks to about 7-fold higher value. Ampicillin concentration was 7.2 mM. For *B* the applied voltage was −100 mV, and membrane-bathing solution was 1 M KCl for *A* and *B*.

The nature of the peak sharpness in Fig. 4*B* is not clear at the moment. One obvious speculation is that the charge distribution on the ampicillin molecule is not the only property that is changed by the bathing solution pH. The charge state of the channel groups also depends on solution acidity; this simultaneous titration of the charge on the channel and on the penetrating molecule leads to an effective cooperativity in antibiotic binding.

The measurements reported above were made at a high salt concentration that was necessary to gain in the amplitude of ampicillin-induced current interruptions and, therefore, to facilitate their observation. If drug interaction with the binding site is of electrostatic origin, the number of blockages should go up with the decreasing salt concentration. Indeed, because of the increasing Debye screening length the electric potential of the site should reach further and capture more drug molecules. Experiments with varying salt concentrations, where noise analysis at the single-channel level rather than direct counting was used, confirmed this expectation.

Fig. 5*A* demonstrates a pronounced increase in the frequency of blockages when KCl concentration is reduced from 1.0 M to 0.01 M. Interestingly, a drug molecule of net zero-charge is effectively "stirred" onto the binding site by electric fields emanating from the charges on the protein molecule. The decreasing ion concentration also promotes stronger binding: a 2-fold increase in the antibiotic residence time at 0.01 M KCl is seen in Fig. 5*B*.

Molecular Dynamics Simulations and Discussion

The crystal structure of several porins to a few Å resolution was solved a decade ago (12, 24, 25). The three-dimensional structure shows three water-filled pores for each trimer, which is the functional unit of the protein in the outer membrane. In each monomer, 16 β-strands span the outer membrane and form a barrel with short turns at the periplasmic side and large loops outside the cell. Unlike the other loops, the third loop, L3, is not exposed at the cell surface but folds into the barrel, forming a constriction zone at half the height of the channel. This loop contributes significantly to the permeability properties of the pore, such as its exclusion limit. Moreover, at the constriction zone, a strong transverse electrostatic field exists that is caused by acidic residues in loop L3 and a cluster of basic residues in the barrel wall opposite the loop. The availability of structural information enormously facilitates the interpretation of results obtained in single-molecule experiments.

It is tempting to postulate that the ampicillin zwitterion simultaneously interacts with the positively and negatively (or partly positively or negatively) charged residues at the constriction zone of the OmpF monomer. This attractive interaction facilitates drug translocation through the narrowest part of the channel compensating for the significant entropy loss. During this translocation, ampicillin completely obstructs the channel and, therefore, temporarily (for less than 1 ms) interrupts current carried by small ions.

A model of such interaction is illustrated in Fig. 6. It shows results of molecular dynamics simulations that predict a possible orientation of the antibiotic molecule within the channel pore.

After a refinement of the pore structure (12), the ampicillin molecule was docked manually inside the channel. The conformation of ampicillin was determined by energy optimization of the solvated drug molecule in its zwitterionic form. Initial positioning of ampicillin was chosen to agree with the main experimental findings that suggest (*i*) the transversal position of the molecule in the constriction zone of the pore to explain the total blockage of the current through a monomer, and (*ii*) strong interactions between ampicillin groups and pore residues to account for a complex that is stable enough to last 1 ms.

Several rounds of energy minimization and molecular dynamics refinements were carried out to optimize the position of ampicillin inside the OmpF monomer. This minimization brings the acid group on the molecule in close contact with the three

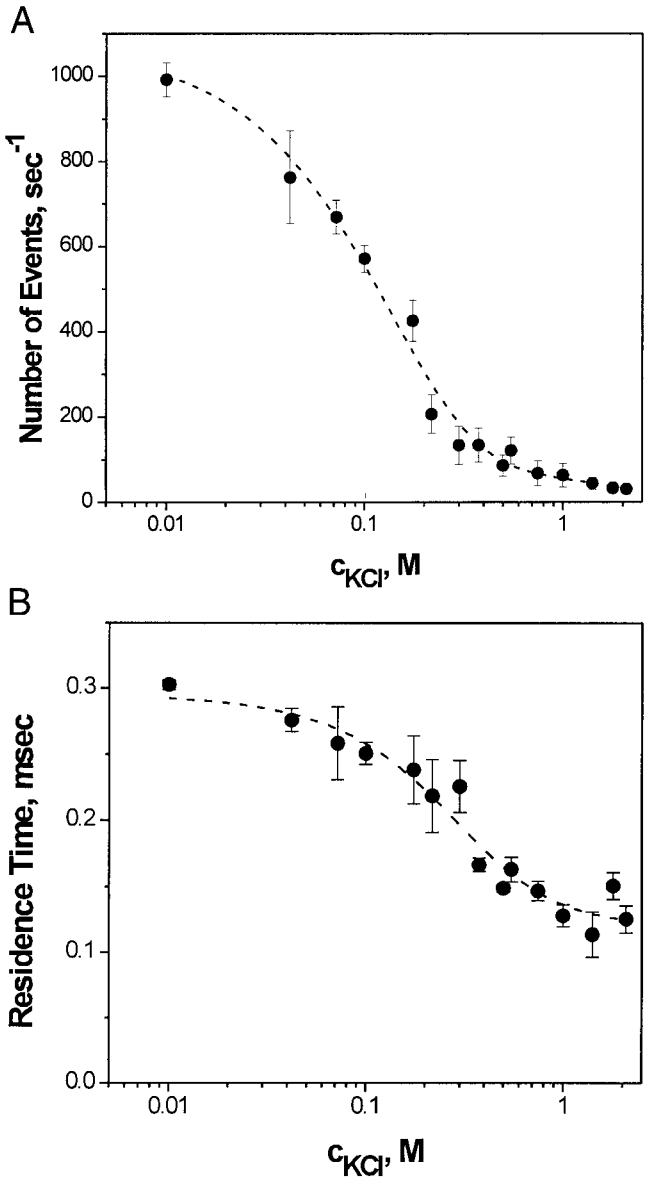

Fig. 5. Kinetic parameters of antibiotic binding as functions of bathing electrolyte concentration. The number of ampicillin-blockage events per second (*A*) as well as ampicillin residence time (*B*) increase with the decreasing KCl concentration. For *A* and *B* the applied voltage was −100 mV, and ampicillin concentration was 5.7 mM, pH 5.0.

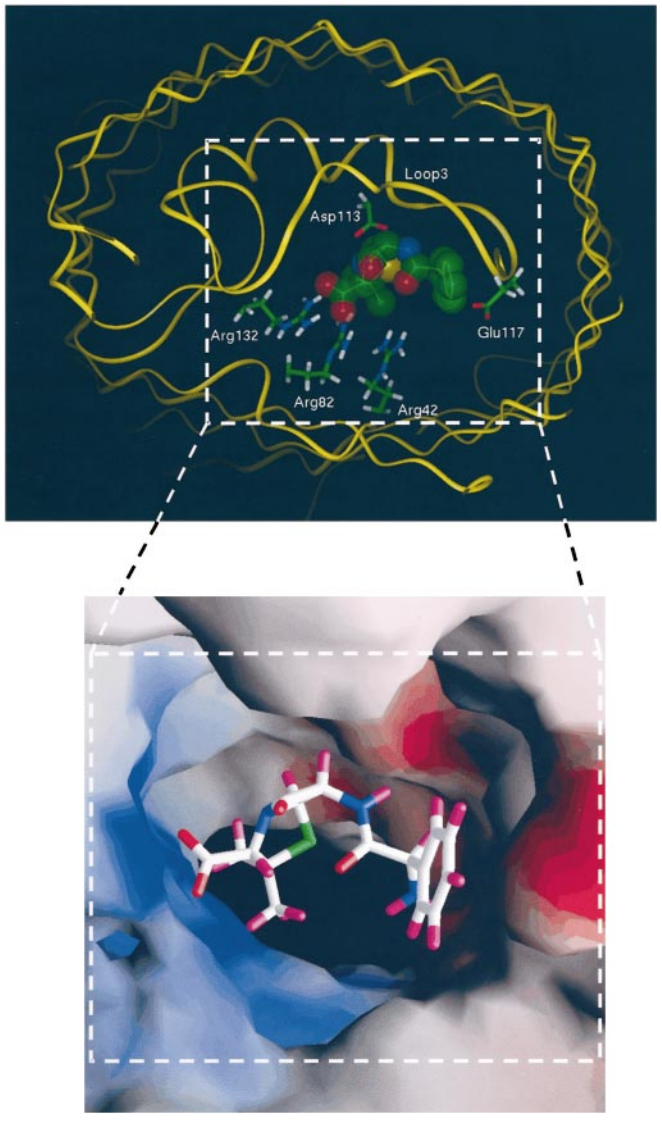

Fig. 6. A model for ampicillin docking in the narrowest part of the OmpF monomeric pore (top view). The zwitterionic ampicillin simultaneously interacts with the positively and negatively charged residues at the constriction zone formed by the β-barrel wall and loop L3. On one side the carboxylate ampicillin group is attracted to the cluster of positively charged residues in the pore, and on the opposite side the ammonium ampicillin group is attracted to the carboxylate of Glu-117. (*Upper*) The skeleton of OmpF is shown in a ribbon representation in yellow. Key residues inside the pore are highlighted with stick representation. The antibiotic molecule is shown as a transparent Corey–Pauling–Koltun model. Green spheres are carbon atoms, red spheres are oxygen atoms, blue spheres are nitrogen atoms, and the yellow sphere is a sulfur atom. Hydrogen atoms of ampicillin are not shown for clarity. (*Lower*) The distribution of the electrostatic potentials of solvent-accessible molecular surface of the OmpF constriction zone complexed with ampicillin is represented with the GRASP program (26). Red zones are negative potentials and blue zones are positive potentials. The ampicillin molecule is represented as a stick model. White sticks are carbon atoms, red sticks are oxygen atoms, blue sticks are nitrogen atoms, the green stick is a sulfur atom, and violet sticks are hydrogen atoms.

clustered arginines (Arg-132, Arg-82, and Arg-42), whereas the ammonium group at the other end of the ampicillin molecule is attracted to Glu-117. In addition, the phenyl group of the ampicillin is stabilized by hydrophobic environment of Tyr-32, Tyr-22, and Phe-118. Molecular modeling reveals a remarkably close fit between the ampicillin molecule and constriction zone dimensions.

The importance of charge distribution on a solute molecule in permeation through OmpF pores has been appreciated for more than a decade. For example, in comparison of zwitterionic vs. monoanionic cephalosporins and penicillins it was shown that the *E. coli* permeability to zwitterionic drugs is about 50–60 times higher than permeability to their monoanionic analogues (27, 28).

Ampicillin is a so-called "drug of choice" for treatment of *E. coli* infections (29). To reveal the possible connection between drug efficacy and the strength of OmpF-antibiotic binding, we probed several other β-lactam antibiotics. Specifically, we studied ceftriaxone, which is known to be a drug of first choice for *E. coli* treatment, and found a pronounced affinity of this drug to OmpF. Statistical analysis of the ceftriaxone-induced current blockages yielded voltage-dependent characteristic times up to

0.5 ms (data not shown). At the same time, in a number of experiments we found an extremely low-strength binding between OmpF and azlocillin, carbenicillin, and piperacillin, antibiotics ineffective for *E. coli* treatment. Importantly, in swelling assay experiments (30) these three drugs were shown to have the lowest "relative diffusion rate."

Conclusions

The permeation barrier alone rarely produces antimicrobial resistance; however, in many cases low membrane permeability works synergistically with other mechanisms of bacterial resistance, such as degradation of antibiotics by periplasmic β-lactamases or active drug efflux (1, 28, 31, 32). Although our study deals only with the initial step in the chain of events involved in the drug action—drug penetration into Gram-negative bacteria—we find a new aspect of structure-function relationship. We show the importance of solute-pore interactions in antibiotic translocation through a bacterial general porin, OmpF.

It is noteworthy that OmpF channels can be reconstituted into artificial polymeric membranes in a fully functional state (33). Such functionalized polymer membranes are mechanically stable and, based on the principles described in this report, can be used in commercial devices for rapid screening of different, newly synthesized compounds.

We are grateful to Adrian Parsegian, Don Rau, and Alexander Berezhkovskii for valuable discussions and comments.

1. Nikaido, H. (1994) *Science* **264,** 382–388.
2. Trnobranski, P. H. (1998) *J. Clin. Nurs.* **7,** 392–400.
3. Ash, C. (1996) *Trends Microbiol.* **4,** 371–372.
4. Rolinson, G. N. (1998) *J. Antimicrob. Chemother.* **41,** 589–603.
5. Nikaido, H. (1989) *Antimicrob. Agents Chemother.* **33,** 1831–1836.
6. Nikaido, H. (1999) in *Escherichia Coli and Salmonella*, ed. Neidhardt, F. C., (Am. Soc. Microbiol., Washington, DC), pp. 29–47.
7. Simonet, V., Mallea, M. & Pages, J. M. (2000) *Antimicrob. Agents Chemother.* **44,** 311–315.
8. Walsh, C. (2000) *Nature (London)* **406,** 775–781.
9. Jeanteur, D., Schirmer, T., Fourel, D., Simonet, V., Rummel, G., Widmer, C., Rosenbusch J. P., Pattus, F. & Pages, J. M. (1994) *Proc. Natl. Acad. Sci. USA* **91,** 10675–10679.
10. Rostovtseva, T. K., Liu, T.-T., Colombini, M., Parsegian, V. A. & Bezrukov, S. M. (2000) *Proc. Natl. Acad. Sci. USA* **97,** 7819–7822.
11. Kullman, L., Winterhalter, M. & Bezrukov, S. M. (2002) *Biophys. J.* **82,** 803–812.
12. Cowan, S. W., Schirmer, T., Rummel, G., Steiert, M., Ghosh, R., Pauptit, R. A., Jansonius, J. N. & Rosenbusch, J. P. (1992) *Nature (London)* **358,** 727–733.
13. Luckey, M. & Nikaido, H. (1980) *Proc. Natl. Acad. Sci. USA* **77,** 167–171.
14. Benz, R., Schmid, A. & Vos-Scheperkeuter, G. H. (1987) *J. Membr. Biol.* **100,** 21–29.
15. Schirmer, T. (1998) *J. Struct. Biol.* **121,** 101–109.
16. Meyer, J. E. W. & Schulz, G. E. (1997) *Protein Sci.* **6,** 1084–1091.
17. Bezrukov, S. M. (2000) *J. Membr. Biol.* **174,** 1–13.
18. Kasianowicz, J. J., Brandin, E., Branton, D. & Deamer, D. W. (1996) *Proc. Natl. Acad. Sci. USA* **93,** 13770–13773.
19. Bayley, H. & Cremer, P. S. (2001) *Nature (London)* **413,** 226–230.
20. Neher, E. & Stevens, C. F. (1977) *Annu. Rev. Biophys. Bioeng.* **6,** 345–381.
21. Rostovtseva, T. K. & Bezrukov, S. M. (1998) *Biophys. J.* **74,** 2365–2373.
22. Hou, J. P. & Poole, J. W. J. (1969) *Pharm. Sci.* **58,** 1510–1515.
23. Rolinson, G. N. & Stevens, S. (1961) *Br. Med. J.* **2,** 191–196.
24. Weiss, M. S., Wacker, T., Weckesser, J., Welte, W. & Schulz, G. E. (1990) *FEBS Lett.* **267,** 268–271.
25. Weiss, M. S., Abele, U., Weckesser, J., Welte, W., Schiltz, E. & Schulz, G. E. (1991) *Science* **254,** 1627–1630.
26. Nicholls, A., Sharp, K. A. & Honig, B. (1991) *Proteins Struct. Funct. Genet.* **11,** 281–296.
27. Nikaido, H., Rosenberg, E. Y. & Foulds, J. (1983) *J. Bacteriol.* **153,** 232–240.
28. Nikaido, H. & Normark, S. (1987) *Mol. Microbiol.* **1,** 29–36.
29. Fairbanks, D. N. F. (2001) *Pocket Guide to Antimicrobial Therapy in Otolaryngology–Head and Neck Surgery* (Am. Acad. Otolaryngol., Alexandria, VA).
30. Yoshimura, F. & Nikaido, H. (1985) *Antimicrob. Agents Chemother.* **27,** 84–92.
31. Hancock, R. E. W. (1997) *Trends Microbiol.* **5,** 37–42.
32. Lakaye, B., Dubus, A., Lepage, S., Groslambert, S. & Frere, J.-M. (1999) *Mol. Microbiol.* **31,** 89–101.
33. Meier, W., Nardin, C. & Winterhalter, M. (2000) *Angew. Chem. Int. Ed. Engl.* **39,** 4599–4602.